

Bandgap engineering using a-Si:H/a-SiN_x:H superlattices

Stefan L. Luxembourg, Peter Kúš and Miro Zeman

Abstract—In order to produce a suitable material for application as barrier layer in hydrogenated amorphous silicon (a-Si:H) based superlattices, thin films of hydrogenated amorphous silicon nitride (a-SiN_x:H) were deposited using plasma enhanced chemical vapor deposition from mixtures of SiH₄ and NH₃ in various ratios. Compositional and optoelectronic properties such as the optical bandgap and chemical bond densities were determined for the resulting series of a-SiN_x:H films. Superlattice structures were fabricated using thin a-SiN_x:H layers as barrier material and a-Si:H layers as well material. Quantum confinement was demonstrated from the observed shift of the optical bandgap to higher energies with decreasing well layer thickness. This effect was successfully modeled using a simple single quantum well model.

Index Terms—amorphous silicon nitride, plasma enhanced chemical vapor deposition, solar cell, and superlattice.

I. INTRODUCTION

Thin-film hydrogenated amorphous silicon (a-Si:H) based solar cells are promising candidates for low-cost photovoltaic energy generation. The main advantage of thin-film a-Si:H solar cells over their crystalline counterparts is the potential reduction in costs when produced in sufficiently large volumes [1]. Further reduction of costs per Watt output power of thin-film solar cells is expected to arise from improvement of their efficiency. Currently, commercially available modules have stabilized efficiencies of 6–7 %. Two important factors, which limit the efficiency of solar cells are thermalization of electrons excited above the material's bandgap and non-absorption of photons with energy smaller than its bandgap. In order to improve the efficiency of solar cells by more efficient use of the solar energy spectrum the concept of tandem (or multi-junction) solar cells is applied. Tandem solar cells combine several single-junction solar cells, in which the absorber materials have different optical bandgaps. The

implementation of the tandem solar cell concept in thin-film silicon technology has led to the development of double and triple-junction thin-film solar cells [2-4]. A stabilized efficiency of 13 % was achieved with a triple junction solar cell, in which the absorber layers were a-Si:H, amorphous silicon-germanium (a-SiGe:H) and microcrystalline silicon (μ c-Si:H) [4]. The bandgaps of a-Si:H and μ c-Si:H are 1.7 and 1.1 eV, respectively. The a-SiGe:H bandgap can be varied between 1.1 and 1.7 eV depending on the germanium content of the material. Although, the energy available from the solar spectrum is more efficiently used in a triple junction solar cell as compared to a single junction a-Si:H cell, still a large part of the solar energy remains unused. Recently, the concept of amorphous silicon based bandgap engineering using superlattices and quantum dots has received considerable attention as a generic approach to further extend the range of materials available to realize solar cells with improved spectrum utilization [5].

Amorphous silicon based superlattices [6-9] consist of alternating layers a-Si:H and one of its alloys. The high band gap material is referred to as the barrier layer, the low bandgap material as the well layer. The electronic band diagram of a superlattice is characterized by periodic repetition of band discontinuities in the both the valence and conduction band. Sufficiently thin well layers cause quantum confinement of charge carriers, which quantizes the allowed energy states, thereby influencing the effective optical bandgap of the superlattice material. This effect was first observed in crystalline semiconductor superlattices [10] and was later found to be present in amorphous superlattices produced using plasma enhanced chemical vapor deposition (PECVD) as well [6-9].

In this work amorphous silicon nitride (a-SiN_x:H) was selected as barrier material for superlattice structures. Since its optical bandgap can be varied over a wide energy range (1.9-5.3 eV) this material has been attractive for application in such structures already from the pioneering work in the 1980s [6-9], [11], [12]. The optical and compositional properties of a-SiN_x:H films deposited from SiH₄ and NH₃ gas mixtures of various ratios were investigated. A-SiN_x:H material with an optical bandgap of 2.85 eV was implemented in a-Si:H/a-SiN_x:H superlattices. The influence of the thickness of the a-Si:H well layer material on the optical properties of the superlattices was studied.

Manuscript received October 1, 2007. This work has been carried out with a subsidy of Dutch Ministry of Foreign Affairs under EOS-LT program and project number EOSLT02028.

Stefan L. Luxembourg is with DIMES-ECTM, Delft University of Technology, P. O. Box 5053, 2600 GB Delft, The Netherlands (phone: +31-15-2787307, fax: +31-15-2622163, email: s.l.luxembourg@tudelft.nl).

Peter Kúš is with The Department of Experimental Physics, FMFI, Comenius University, SK-842 15 Bratislava, Slovakia (email: kus@fmph.uniba.sk).

Miro Zeman is with DIMES-ECTM, Delft University of Technology, P. O. Box 5053, 2600 GB Delft, The Netherlands (email: m.zeman@tudelft.nl).

II. EXPERIMENTAL

A-SiN_x:H films were prepared by rf PECVD from a gas mixture of SiH₄ and NH₃ in the AMOR deposition system in a reaction chamber equipped with a showerhead electrode. The nitrogen content in the alloys was controlled by varying the fraction of NH₃ in the total gas mixture: %NH₃ = ([NH₃] / ([NH₃] + [SiH₄])) × 100 % from 6 to 96 %. The films were deposited with an rf power density of 34 mW/cm², an inter-electrode distance of 14 mm, a deposition pressure of 80 Pa and a substrate temperature of 235 °C. Thicknesses of the deposited films were around 300 nm. Corning Eagle 2000™ glass, quartz and silicon wafer were used as substrates.

Superlattice samples were prepared on Corning glass substrates by sequential deposition of a-Si:H and a-SiN_x:H layers without interrupting the plasma upon changing the gas mixture. From an estimate of the residence time of the gas in the deposition chamber it can be predicted whether abrupt interfaces can be grown using this approach. The residence time (T_R) can be calculated from Eq. 1:

$$T_R = \frac{V \cdot p}{F_0 \cdot p_0} \quad (1)$$

in which V is the volume of the reactor chamber, p the deposition gas pressure and F_0 the flow rate at standard pressure (p_0). When only the inter-electrode volume is taken into account (~ 1 liter), the residence time is estimated to be close to 1 s for the above mentioned deposition conditions. The residence time of 1 s is significantly less than the time needed to grow a monolayer ($\sim 2 - 3$ s). Therefore, it can be expected that multilayer samples with well-defined interfaces can be deposited without interrupting the plasma.

Reflection and transmission (RT) spectra were recorded in the 200–1200 nm spectral range using a Perkin–Elmer 900 spectrophotometer. The thin films' refractive index, n , absorption coefficient, α , and thickness were derived from fitting of the obtained spectra using the interband transition model by O'Leary, Johnson and Lim (OJL) [13] as implemented in the SCOUT 2.1! software package [14].

The appearance of the superlattice RT spectra results from the combined dielectric properties of the well and barrier layer materials. In order to determine the well layer absorption coefficient, α_w , we adapted the effective medium formalism described by Ugur and Johanson [15]. For this purpose an effective dielectric constant ϵ^* was obtained from OJL modeling of the recorded RT spectra. According to formalism mentioned above this ϵ^* can be related to the well and barrier dielectric constants: ϵ_w and ϵ_B , respectively, via [15]:

$$\epsilon^* d = \epsilon_w N_w d_w + \epsilon_B N_B d_B \quad (2)$$

in which d , d_w and d_B are, respectively, the total film thickness, the well layer thickness and the barrier layer thickness, N_w the number of well layers and N_B the number of barrier layers.

From a separate RT measurement of a bulk a-SiN_x:H sample with the same composition as the barrier layer material the ϵ_B can be determined. When the thicknesses are known (see below) ϵ_w can be determined. Now, α_w can be determined from the complex part of ϵ_w .

The ratios of the atomic concentration of nitrogen over silicon ($x = [N]/[Si]$) in the thin films were estimated using an approach proposed by Bustarret *et al.* [16]. In this method the refractive index of a-SiN_x:H alloys is related to a linear combination of the reference refractive indices taken at $x = 0$ (a-Si:H) and $x = 1.33$ (a-Si₃N₄:H, stoichiometric silicon nitride) weighted by the [Si–N] and [Si–Si] bond densities, respectively [17]. Therefore, the x can be obtained from the refractive index of the a-SiN_x:H material using Eq. 2 [16]:

$$x = \frac{[N]}{[Si]} = \frac{4}{3} \frac{n_{a-Si:H} - n}{n + n_{a-Si:H} - 2n_{a-Si_3N_4:H}} \quad (3)$$

with the refractive indices at 632.8 nm. For the reference refractive indices of a-Si:H and a-Si₃N₄:H we used the experimentally derived values of 4.29 and 1.83, respectively.

The nature and concentration of the chemical bonds present in the a-SiN_x:H films were determined from infrared spectra (400–4000 cm⁻¹) obtained using a Thermo Nicolet 5700 Fourier Transform Infrared (FTIR) Spectrometer. The [Si–H] and [N–H] bond densities were determined from the normalized 2160 cm⁻¹ and 3340 cm⁻¹ absorption bands according to Eq. 4:

$$N_{X-Y} = K_{X-Y} \int \alpha(\nu) d\nu \quad (4)$$

with the integral taken over the full absorption band and where N_{X-Y} is the density of X-Y bonds and K_{X-Y} the corresponding extinction coefficient for this particular absorption band. The extinction coefficients used were determined by Lanford and Rand [18]: $K_{Si-H} = 5.9 \times 10^{16}$ cm⁻¹ and $K_{N-H} = 8.2 \times 10^{16}$ cm⁻¹, for the bands at 2160 cm⁻¹ and 3340 cm⁻¹, respectively.

The layered structure and the individual barrier and well layer thicknesses of the superlattice films were studied using Transmission Electron Microscopy (TEM).

III. RESULTS

A. a-SiN_x:H thin films

The thicknesses of the a-SiN_x films were determined from the RT spectra. The corresponding deposition rates are included in Fig. 1A as a function of %NH₃. The deposition rate increases from ~ 1 Å/s for low NH₃ gas flows to approximately 1.8 Å/s for %NH₃ of 50 % and higher.

As explained in the experimental section (Eq. 3) the nitrogen incorporation into the films can be estimated from the material's refractive index at 632.8 nm. In Fig. 1B the

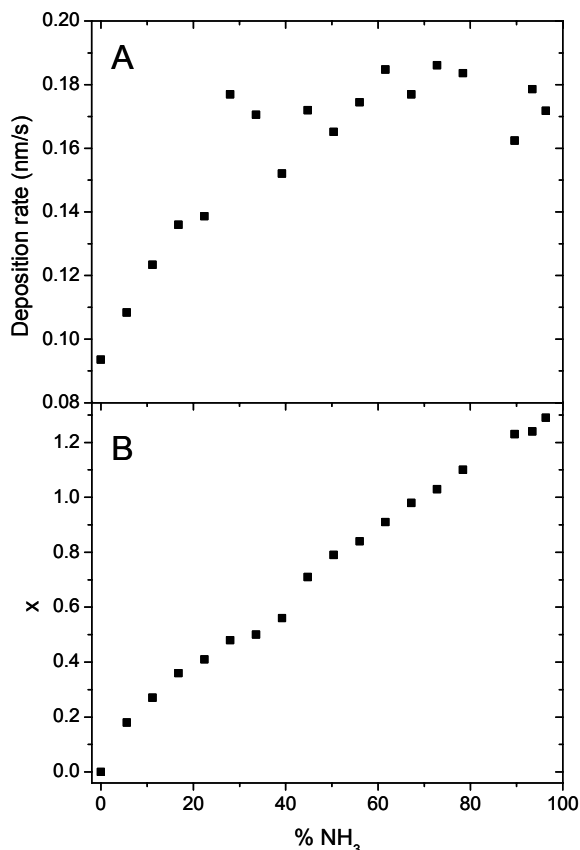


Fig. 1. (A) Deposition rate of a-Si_xN_x:H films and (B) Nitrogen incorporation in the films versus %NH₃ in the deposition gas mixture.

[N]/[Si] ratio is shown as a function of the %NH₃. The nitrogen incorporation increases linearly from zero for a-Si:H to close to the stoichiometric value ($x = 1.33$) for a 96 % NH₃ gas mixture. In Fig. 2 the E_{04} bandgap, defined as the energy for which α equals 10^4 cm^{-1} is plotted as a function of x . In agreement with earlier studies [19], [20] it is found that the optical bandgap increases linearly from 1.9 to 2.9 eV for values of x ranging from 0 to 1. Above $x = 1$ the bandgap increases rapidly to a value of 5.3 eV for stoichiometric silicon nitride [19]. According to Robertson [21] the value of $x \approx 1$ corresponds to the transition from a silicon-like region to a transition region. In the silicon-like regime extended networks of Si-Si bonds with embedded Si-N clusters exist, while for $x > 1$ the silicon - nitrogen network becomes dominant and the optical gap is controlled by Si-N and N-H bonds. The a-Si_xN_x:H IR spectra in the range of 400-4000 cm^{-1} contain contributions from vibrational modes of three types of bonds: Si-H, Si-N and N-H. The different IR absorption modes have been identified in earlier publications [16], [22], [23] and were observed for the films studied in the present work as well. IR absorption modes related to N-H bonds were detected around 3340 cm^{-1} (stretching), 1550 cm^{-1} (H-N-H bending) and 1180 cm^{-1} (bending). Si-H stretching modes were observed around 2100 cm^{-1} , Si-N stretching near 840 cm^{-1} and Si-N breathing at 480 cm^{-1} . Fig. 3 shows IR spectra of a-

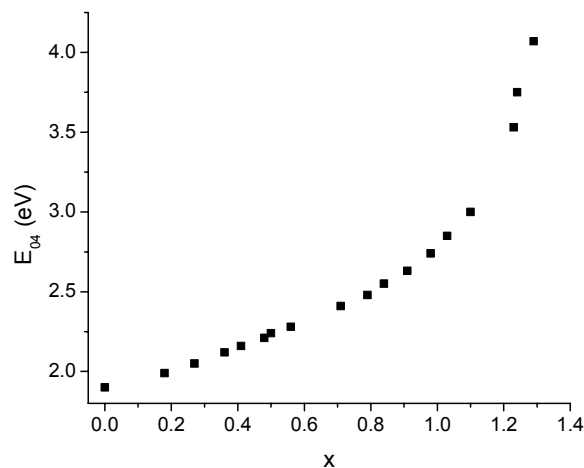


Fig. 2. The E_{04} optical bandgap as a function of $x = [\text{N}]/[\text{Si}]$; $x = 1$ marks the change from a Si-Si to a Si-N dominated network.

Si_xN_x:H films for three indicated values of x . The spectra were corrected for interference effects via baseline subtraction.

In Fig. 4A it is shown that the peak position of the Si-H stretching peak shifts with increasing nitrogen content from around 2070 cm^{-1} to about 2160 cm^{-1} . This observation is in line with the high wavenumber assignment of Si-H bond vibrations involving Si atoms bound to (multiple) N atoms: 2005 cm^{-1} (Si₃Si-H), 2065 cm^{-1} (Si₂Si-H₂), 2082 cm^{-1} (NSi₂Si-H), 2140 cm^{-1} (NSiSi-H₂, N₂SiSi-H), 2175 cm^{-1} (N₂Si-H₂), 2220 cm^{-1} (N₃Si-H) [16].

The Si-N stretching vibrations peak centered around 840 cm^{-1} can be deconvoluted into multiple vibrational modes. In total four different modes were identified by Gaussian fitting of the spectra (not shown). Earlier studies of the Si-N IR modes yielded either three [24], [25] or four modes [16]. In references [24] and [25] the 930 cm^{-1} and 990 cm^{-1} modes are replaced by a single 960 cm^{-1} mode. The band at 750 cm^{-1} is usually assigned to in-plane stretching vibration of isolated Si-N bonds in a Si-network [16], [25]. Assignment of the other

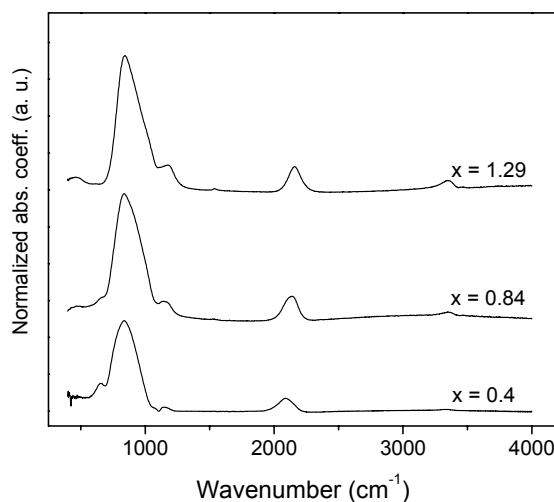


Fig. 3. Evolution of the IR a-Si_xN_x:H IR spectrum with increasing N content. For assignment of the different IR absorption modes see text.

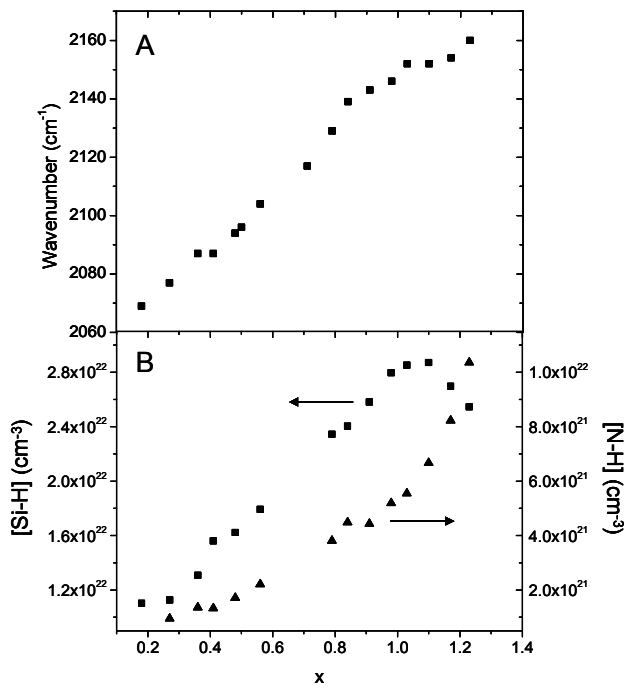


Fig. 4. (A) Shift of the Si-H stretch peak position. (B) Si-H bond densities (squares) and N-H bond densities (triangles) as determined from the IR absorption bands at 2100 cm^{-1} and 3340 cm^{-1} , respectively.

contributions to the Si-N stretching band is less straightforward. According to Lucovsky et al. [25] this mode shifts to 830-840 cm^{-1} for the N site, which has at least one H atom as second neighbor. In contrast, Della Salla et al. [26] assumed that the 840 cm^{-1} and 960 cm^{-1} modes arise from Si-N(Si_2) and Si-NH-Si, respectively. In this present work, we find that for values of $x < 0.5$ the S-N stretching band is best fitted with three Gaussian contributions at: 750 cm^{-1} , 830 cm^{-1} and 930 cm^{-1} , if x is increased above 0.5 an additional Gaussian centered at 990 cm^{-1} is needed. For increasing nitrogen content the 750 cm^{-1} component gradually reduces, for $x > 0.7$ this absorption mode has completely disappeared. This observation agrees with the earlier assignment of the 750 cm^{-1} mode to isolated Si-N bonds, namely with increasing x Si-Si bonds are increasingly replaced by Si-N bonds resulting in a continuous Si-N network.

The [Si-H] and [N-H] bond densities can be calculated from the Si-H and N-H stretching absorption bands using the method detailed in the experimental section (Eq. 4). In Fig. 4B the resulting bond densities are shown as function of the nitrogen content of the films. The sum of the two bond densities can be used to estimate the total hydrogen content in the film. Clearly, with increasing nitrogen content, below $x = 1$, the hydrogen content of the film is increased mainly by the replacement of Si-Si bonds by Si-H bonds. For nitrogen rich films ($x > 1$) the [Si-H] bond density decreases sharply, while the [N-H] bond density increase becomes steeper. At these high nitrogen contents a contribution to the spectrum at 3450 cm^{-1} becomes noticeable (not shown). This has been assigned to the H-N-H stretching mode [27]. In this range part of the

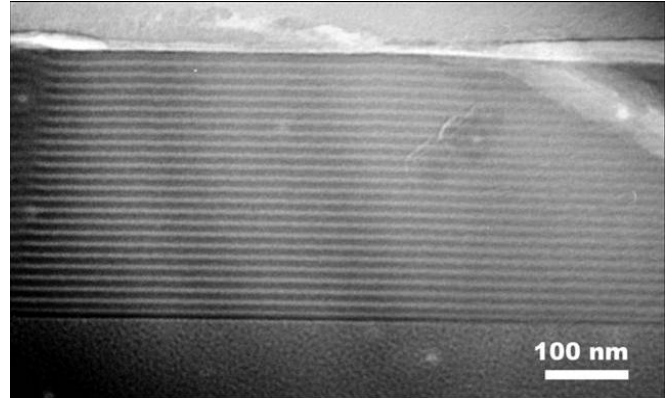


Fig. 5. TEM image of a superlattice sample. The light layers correspond to a-Si $_x$:H.

Si-Si and Si-H bonds are replaced by Si-NH $_n$ groups. From the results of IR spectroscopy we can summarize the compositional properties of the a-Si $_x$:H films, which correspond to the general view on nitrogen incorporation into the Si-Si network. In the films with $x < 1$ a continuous Si-Si network exists, with increasing x Si-Si bonds are steadily replaced by Si-N and Si-H bonds. For $x < 0.7$ isolated Si-N bonds are still detected in the films. For films with $x > 1$ the Si-N network becomes dominant and Si-H bonds are replaced by N-H bonds, which results in a decrease of the film's hydrogen content for values of x close to 1.33 [27].

B. Superlattices

Superlattice samples were fabricated by alternating deposition of a-Si:H and a-Si $_x$:H layers. For this purpose a-Si $_x$:H grown from a deposition gas mixture of 75% NH_3 and 25% SiH_4 was used. This material is characterized by an E_{04} bandgap of 2.85 eV and an [N]/[Si] ratio of approximately 1. For the series of superlattices the thickness of the barrier layer was kept constant while the well layer thickness was varied from 1 – 25 nm. Bulk deposition rates were used to determine the required process times to arrive at the desired thicknesses. The actual barrier and well layer thicknesses were determined by TEM analysis. In Fig. 5 an example of a TEM recording of the layered structure of a multilayer sample is shown. The TEM image reveals a high quality, regular layer stack. For this particular example the thickness of the a-Si:H layer was determined to be 9.8 nm, the a-Si $_x$:H thickness was 4.4 nm.

RT spectroscopy was used to determine the absorption spectra of the superlattice samples. As explained in the experimental section the α_w can be obtained using the effective medium expression (Eq. 2). The resulting absorption curves are included in Fig. 6A together with a-Si:H and a-Si $_x$:H bulk absorption curves. From these results a shift of the optical bandgap to higher energies with decreasing well layer thickness is apparent. This effect becomes most pronounced at thicknesses of 5 nm and below, which is in agreement with earlier work [6], [8], [11]. The observed shift of the optical bandgap can be attributed to quantum confinement of the charge carriers: for small well layer thicknesses and barriers of

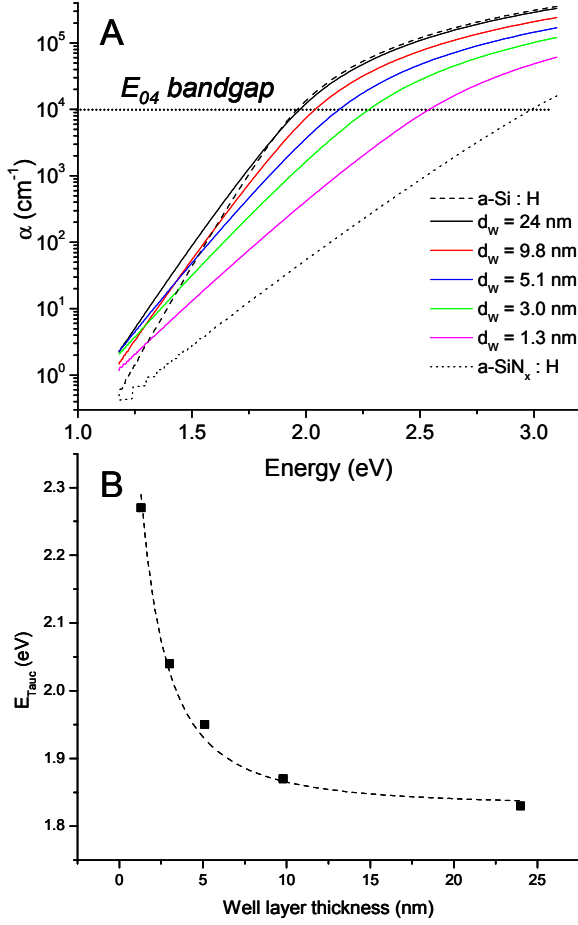


Fig. 6. (A) The superlattice absorption spectra demonstrate a clear blueshift for decreasing thickness of the well layer. A-Si:H and a-SiN_x:H ($x \approx 1$) bulk absorption spectra are also included. (B) The experimentally determined Tauc bandgaps of the superlattice samples (squares) can be modeled by a simple single quantum well model (dashed line).

the appropriate height the allowed energy levels become quantized, which results in a shift of the lowest allowed energy state.

From a Tauc plot [28] of the absorption data the Tauc optical bandgap can be derived. In Fig. 6B the Tauc optical bandgaps of the different superlattices are plotted against the well layer thickness. The change in optical bandgap can be reproduced by a simple quantum well model [6]. According to this model confinement of an electron (hole) with effective mass m^* (m_H^*) in a one-dimensional well with depth U and width d increases its ground state energy by an amount ΔE which is the lowest order solution of Eq. 5:

$$\cos\left(\frac{k \cdot d}{2}\right) = \frac{k}{Q} \quad (5)$$

with d , the well layer thickness, $k = (2m^*\Delta E)^{1/2}/\hbar^2$ and $Q = (2m^*U)^{1/2}/\hbar^2$, in which \hbar is the Dirac constant. This expression assumes that the coupling between adjacent wells is negligible. If the band discontinuities are assumed to be distributed equally over the valence and conduction bands and

the hole mass equal to the free electron mass, the effective electron mass is the only fitting parameter in the model. The best fit, obtained for $m^* = 0.1 m_0$ is included in Fig. 6B. Since the value of m^* is highly dependent on the choice of distribution of the band discontinuity this result has no physical significance. It serves to show the consistency of the Tauc optical bandgap shift with quantum size effects.

IV. CONCLUSION

A-SiN_x:H thin films were deposited from different SiH₄ and NH₃ mixing ratios. RT and FTIR spectroscopy were used to investigate the effect of nitrogen incorporation into the Si-Si network on the optical bandgap and bond densities. Superlattices structures were deposited with a-Si:H as the well layer and a-SiN_x:H with an E_{04} bandgap of 2.85 eV and $x \approx 1$ as the barrier layer. Decreasing the well layer thickness below 5 nm resulted in a strong blueshift of the absorption spectra which has been attributed to the confinement of charge carriers.

REFERENCES

- [1] S. Hegedus, "Thin film solar modules: the low cost, high throughput and versatile alternative to Si wafers," *Progress Photovoltaics*, vol. 14, pp. 393-411, 2006.
- [2] J. Meier, S. Dubail, J. Cuperus, U. Kroll, R. Platz, P. Torres, J. A. Anna Selvan, P. Pernet, N. Beck, N. Pellaton Vaucher, C. Hof, D. Fischer, H. Keppner, and A. Shah, "Recent progress in micromorph solar cells," *J. Non-Cryst. Solids*, vol. 227-230, pp. 1250-1256, 1998.
- [3] K. Yamamoto, M. Yoshimi, Y. Tawada, Y. Okamoto, and A. Nakajima, "Thin film Si solar cell fabricated at low temperature," *J. Non-Cryst. Solids*, vol. 266-269, pp. 1082-1087, 2000.
- [4] J. Yang, A. Banerjee, and S. Guha, "Triple-junction amorphous silicon alloy solar cell with 14.6% initial and 13.0% stable conversion efficiencies," *Appl. Phys. Lett.*, vol. 70, pp. 2975 - 2977, 1997.
- [5] G. Conibeer, M. Green, R. Corkish, Y. Cho, E.-C. Cho, C.-W. Jiang, T. Fangsuwannarak, E. Pink, Y. Huang, T. Puzzer, T. Trupke, B. Richards, A. Shalav, and K.-I. Lin, "Silicon nanostructures for third generation photovoltaic solar cells," *Thin Solid Films*, vol. 511-512, pp. 654-662, 2006.
- [6] B. Abeles and T. Tiedje, "Amorphous Semiconductor Superlattices," *Phys. Rev. Lett.*, vol. 51, pp. 2003-2006, 1983.
- [7] M. Hirose and S. Miyazaki, "Luminescence and transport in a-Si:H/a-Si_{1-x}N_x:H quantum well structures," *J. Non-Cryst. Solids*, vol. 66, pp. 327-338, 1984.
- [8] N. Ibaraki and H. Fritzsche, "Properties of amorphous semiconducting a-Si:H/a-SiN_x:H multilayer films and of a-SiN_x:H alloys," *Phys. Rev. B*, vol. 30, pp. 5791-5799, 1984.
- [9] J. Kakalios, H. Fritzsche, N. Ibaraki, and S. R. Ovshinsky, "Properties of amorphous semiconducting multilayer films," *J. Non-Cryst. Solids*, vol. 66, pp. 339-344, 1984.
- [10] L. Esaki and R. Tsu, "Superlattice and Negative Differential Conductivity in Semiconductors," *IBM J. Res. Develop.*, vol. 14, pp. 61 - 65, 1970.
- [11] S. Kalem, "Optical investigation of a-Si:H/a-SiN_x:H superlattices," *Phys. Rev. B*, vol. 37, pp. 8837-8841, 1988.
- [12] M. Yamaguchi, H. Ohta, C. Ogihara, H. Yokomichi, K. Morigaki, S. Nonomura, and S. Nitta, "Gap states and recombination processes in one-dimensionally ordered and disordered a-Si:H/a-Si_{1-x}N_x:H multilayer films," *J. Non-Cryst. Solids*, vol. 97-98, pp. 931-934, 1987.

- [13] S. K. O'Leary, S. R. Johnson, and P. K. Lim, "The relationship between the distribution of electronic states and the optical absorption spectrum of an amorphous semiconductor: An empirical analysis," *J. Appl. Phys.*, vol. 82, pp. 3334 - 3340, 1997.
- [14] W. Theiss, "SCOUT!," 2.1 ed Aachen, Germany: M. Theiss Hard- and Software.
- [15] H. Ugur, R. Johanson, and H. Fritzsche, "Effective medium expression for the optical properties of periodic multilayer films," in *Tetrahedrally Bonded Amorphous Semiconductors*, D. Adler and H. Fritzsche, Eds. New York: Plenum, 1985, pp. 425-431.
- [16] E. Bustarret, M. Bensouda, M. C. Habrard, J. C. Bruyère, S. Poulin, and S. C. Gujrathi, "Configurational statistics in a-Si_xN_yH_z alloys: A quantitative bonding analysis," *Phys. Rev. B*, vol. 38, p. 8171, 1988.
- [17] T. Makino, "Composition and Structure Control by Source Ratio in LPCVD SiN_x," *J. Electrochem. Soc.*, vol. 130, pp. 450-455, 1983.
- [18] W. A. Lanford and M. J. Rand, "The hydrogen content of plasma deposited silicon nitride," *J. Appl. Phys.*, vol. 49, pp. 2473-2477, 1978.
- [19] F. Giorgis, C. F. Pirri, and E. Tresso, "Structural properties of a-Si_{1-x}N_x:H films grown by plasma enhanced chemical vapour deposition by SiH₄ + NH₃ + H₂ gas mixtures," *Thin Solid Films*, vol. 307, pp. 298-305, 1997.
- [20] E. A. Davis, N. Piggins, and S. C. Bayliss, "Optical properties of amorphous SiN_x(:H) films," *J. Phys. C: Solid State Phys.*, vol. 20, pp. 4415-4427, 1987.
- [21] J. Robertson, "Electronic structure of silicon nitride," *Phil. Mag. B*, vol. 63, pp. 47-77, 1991.
- [22] A. Morimoto, Y. Tsujimura, M. Kumeda, and T. Shimizu, "Properties of Hydrogenated Amorphous Si-N Prepared by Various Methods," *Jap. J. Appl. Phys.*, vol. 24, pp. 1394-1398, 1985.
- [23] C. Senemaud, A. Gheorghiu, L. Amoura, R. Etemadi, H. Shirai, C. Godet, M. Fang, and S. Gujrathi, "Local order and H-bonding in N-rich amorphous silicon nitride," *J. Non-Cryst. Solids*, vol. 164-166, pp. 1073-1076, 1993.
- [24] S. Hasegawa, L. He, Y. Amano, and T. Inokuma, "Analysis of SiH and SiN vibrational absorption in amorphous SiN_x:H films in terms of a charge-transfer model," *Phys. Rev. B*, vol. 48, pp. 5315-5325, 1993.
- [25] G. Lucovsky, J. Yang, S. S. Chao, J. E. Tyler, and W. Czubytyj, "Nitrogen-bonding environments in glow-discharge-deposited a-Si:H films," *Phys. Rev. B*, vol. 28, pp. 3234-3240, 1983.
- [26] D. D. Sala, C. Coluzza, G. Fortunato, and F. Evangelisti, "Infrared and optical study of a-SiN alloys," *J. Non-Cryst. Solids*, vol. 77-78, pp. 933-936, 1985.
- [27] F. Demichelis, F. Giorgis, and C. F. Pirri, "Compositional and structural analysis of hydrogenated amorphous silicon-nitrogen alloys prepared by plasma-enhanced chemical vapor deposition," *Phil. Mag. B*, vol. 74, pp. 155-168, 1996.
- [28] J. Tauc, "Absorption Edge and Internal Electric Fields in Amorphous Semiconductors," *Mat. Res. Bull.*, vol. 5, pp. 721-730, 1970.